THE JOURNAL OF BIOLOGICAL CHEMISTRY VOL. 284, NO. 18, pp. 11863–11872, May 1, 2009

Novel Role of RanBP9 in BACE1 Processing of Amyloid Precursor Protein and Amyloid β Peptide Generation*[S]

Received for publication, September 22, 2008, and in revised form, February 23, 2009 Published, JBC Papers in Press, February 27, 2009, DOI 10.1074/jbc.M807345200

Madepalli K. Lakshmana[‡], Il-Sang Yoon[‡], Eunice Chen[‡], Elizabetta Bianchi[§], Edward H. Koo[‡], and David E. Kang[‡¶1]

From the [‡]Department of Neurosciences, University of California, San Diego, La Jolla, California 92093, [¶]the World Class University Neurocytomics Program, Seoul National University College of Medicine, 28 Yungun-dong, Jongro-gu, Seoul 110-799, Korea, and [§]the Laboratory of Immunoregulation, Department of Immunology, Institut Pasteur, 25 rue du Dr. Roux, 75724 Paris, France

Accumulation of the amyloid β (Aβ) peptide derived from the proteolytic processing of amyloid precursor protein (APP) is the defining pathological hallmark of Alzheimer disease. We previously demonstrated that the C-terminal 37 amino acids of lipoprotein receptor-related protein (LRP) robustly promoted Aβ generation independent of FE65 and specifically interacted with Ran-binding protein 9 (RanBP9). In this study we found that RanBP9 strongly increased BACE1 cleavage of APP and Aβ generation. This pro-amyloidogenic activity of RanBP9 did not depend on the KPI domain or the Swedish APP mutation. In cells expressing wild type APP, RanBP9 reduced cell surface APP and accelerated APP internalization, consistent with enhanced β-secretase processing in the endocytic pathway. The N-terminal half of RanBP9 containing SPRY-LisH domains not only interacted with LRP but also with APP and BACE1. Overexpression of RanBP9 resulted in the enhancement of APP interactions with LRP and BACE1 and increased lipid raft association of APP. Importantly, knockdown of endogenous RanBP9 significantly reduced Aβ generation in Chinese hamster ovary cells and in primary neurons, demonstrating its physiological role in BACE1 cleavage of APP. These findings not only implicate RanBP9 as a novel and potent regulator of APP processing but also as a potential therapeutic target for Alzheimer disease.

The major defining pathological hallmark of Alzheimer disease (AD)[2] is the accumulation of amyloid β protein (Aβ), a neurotoxic peptide derived from β- and γ-secretase cleavages of the amyloid precursor protein (APP). The vast majority of APP is constitutively cleaved in the middle of the Aβ sequence by α-secretase (ADAM10/TACE/ADAM17) in the non-amyloidogenic pathway, thereby abrogating the generation of an intact Aβ peptide. Alternatively, a small proportion of APP is cleaved in the amyloidogenic pathway, leading to the secretion of Aβ peptides (37–42 amino acids) via two proteolytic enzymes, β- and γ-secretase, known as BACE1 and presenilin, respectively (1).

The proteolytic processing of APP to generate Aβ requires the trafficking of APP such that APP and BACE1 are brought together in close proximity for β-secretase cleavage to occur. We and others have shown that the low density lipoprotein receptor-related protein (LRP), a multifunctional endocytosis receptor (2), binds to APP and alters its trafficking to promote Aβ generation. The loss of LRP substantially reduces Aβ release, a phenotype that is reversed when full-length (LRP-FL) or truncated LRP is transfected in LRP-deficient cells (3, 4). Specifically, LRP-CT lacking the extracellular ligand binding regions but containing the transmembrane domain and the cytoplasmic tail is capable of rescuing amyloidogenic processing of APP and Aβ release in LRP deficient cells (3). Moreover, the LRP soluble tail (LRP-ST) lacking the transmembrane domain and only containing the cytoplasmic tail of LRP is sufficient to enhance Aβ secretion (5). This activity of LRP-ST is achieved by promoting APP/BACE1 interaction (6), although the precise mechanism is unknown. Although we had hypothesized that one or more NP*X*Y domains in LRP-ST might underlie the pro-amyloidogenic processing of APP, we recently found that the 37 C-terminal residues of LRP (LRP-C37) lacking the NP*X*Y motif was sufficient to robustly promote Aβ production independent of FE65 (7). Because LRP-C37 likely acts by recruiting other proteins, we used the LRP-C37 region as bait in a yeast two-hybrid screen, resulting in the identification of 4 new LRP-binding proteins (7). Among these, we focused on Ran-binding protein 9 (RanBP9) in this study, which we found to play a critical role in the trafficking and processing of APP. RanBP9, also known as RanBPM, acts as a multi-modular scaffolding protein, bridging interactions between the cytoplasmic domains of a variety of membrane receptors and intracellular signaling targets. These include Axl and Sky (8), MET receptor protein-tyrosine kinase (9), and β2-integrin LFA-1 (10). Similarly, RanBP9 interacts with Plexin-A receptors to strongly inhibit axonal outgrowth (11) and functions to regulate cell morphology and adhesion (12, 13). Here we show that RanBP9 robustly promotes BACE1 processing of APP and Aβ generation.

* This work was supported, in whole or in part, by National Institutes of Health Grant AG 005131-24S1 (NIA, to D. E. K.). This work was also supported in part by the American Health Assistance Foundation Grant A2007-05 (to D. E. K.) and Alzheimer's Association Grant NIRG-07-60584 (to M. K. L.).

[S] The on-line version of this article (available at http://www.jbc.org) contains supplemental Figs. S1–S4.

[1] To whom correspondence should be addressed: Dept. of Neurosciences 0691, UC San Diego, Leichtag Biomedical Research 3A17, 9500 Gilman Dr., La Jolla, CA 92093. Tel.: 858-822-6484; Fax: 858-822-1021; E-mail: dekang@ucsd.edu.

[2] The abbreviations used are: AD, Alzheimer disease; Aβ, amyloid β protein; APP, amyloid precursor protein; sAPP, soluble APP; LRP, low density lipoprotein receptor-related protein; CHO, Chinese hamster ovary; HEK, human embryonic kidney; N2a, Neuro-2a; CHAPS, (3-[(3-cholamidopropyl) dimethylammonio]-2-hydroxy-1-propanesulfonate); ELISA, enzyme-linked immunosorbent assay; CTF, C-terminal fragment; PRD, proline-rich domain; FL, full-length; ST, soluble tail; RanBP9, Ran-binding protein 9; HA, hemagglutinin; PBS, phosphate-buffered saline; siRNA, small interfering RNA; PRD, proline-rich domain; SPRY, SPIa and the ryanodine receptor.

MATERIALS AND METHODS

DNA Constructs—The HA-tagged LRP-L4 mini-receptor variants were subcloned into the retroviral vector pLHCX (Clontech, Palo Alto, CA). LRP-L4 mini-receptor (pLNCX-LRP-L4) was a kind gift from Dr. Marilyn Farquhar. HA-LRP-L4-ΔC37 lacking the last 37 residues of LRP was generated by site-directed mutagenesis (QuikChange, Stratagene, La Jolla, CA). pcDNA-P3X-FLAG-RanBP9 construct was a kind gift from Dr. Shim S-K (Yale University School of Medicine). The deletion mutants of FLAG-tagged RanBP9, Δ1 (expressing amino acids 1–392), Δ2 (expressing 408–729), Δ3 (expressing 1–107), and Δ4 (expressing 1–254) were generated by restriction digestion followed by filling with *Pfu* polymerase and re-ligation in pcDNA-P3X-FLAG vector. All of these cDNAs were sequenced and transferred by restriction digest to the pLHCX vector (Clontech) for retrovirus production.

Chemicals and Antibodies—The polyclonal antibody 1704 recognizes the cytoplasmic domain of human LRP. The polyclonal antibody CT15 (against C-terminal 15 residues of APP) and B279 (against BACE1) and the monoclonal antibodies 1G7 (against APP ectodomain), 26D6 (against 1–16 of Aβ), and Ab9 (against 1–16 of Aβ) have been described previously (5, 6). Monoclonal antibodies 9E10 (against Myc; Calbiochem), Ab-1 (against the β-tubulin; Calbiochem) M2 (anti-FLAG; Sigma), flotillin-1 (against flotillin-1; Santa Cruz Biotechnology), 82E1 (against N terminus of Aβ; IBL, Japan), 6E10 (against 1–17 of Aβ; Covance Research), anti-biotin (Jackson ImmunoResearch), anti-sAPPβ (IBL-America), and anti-Swe-sAPPβ (clone 6A1, IBL-America) were purchased from the indicated vendors. All secondary antibodies were purchased from Jackson ImmunoResearch laboratories (West Grove, PA). Anti-RanBP9 monoclonal antibody was produced by immunizing mice with a peptide corresponding to 146–729 amino acids of RanBP9 (10). All antibodies were diluted in 5% fat-free milk in Tris-buffered saline-Tween buffer. Hygromycin B and Geneticin were purchased from Invitrogen, EZ-Link Sulfo-NHS-LC-Biotin was from Pierce, and anti-mouse IgG and anti-rabbit IgG-agarose beads were from American Qualex International.

Cell Cultures and Generation of Stable Cell Lines—Chinese hamster ovary (CHO), human embryonic kidney (HEK) 293T, and Neuro-2a (N2a) cells were grown in Dulbecco's modified Eagle's medium containing 10% fetal bovine serum, 2 mM L-glutamine, 100 μg/ml penicillin, and 100 μg/ml streptomycin. CHO-APP751, CHO-APP695, N2a-APP751, and N2a-Swe-APP695 cells stably expressing FLAG-RanBP9 variants were generated by retroviral transduction as previously described (6). Briefly, 293HP cells were transiently co-transfected with vesicular stomatitis virus glycoprotein and pLHCX-RanBP9 variant constructs, and conditioned medium collected over a 48-h period was used to transduce the cells and selected with 500 μg/ml hygromycin. Stable cells were then maintained with 100 μg/ml hygromycin B.

Cell/Tissue Extraction and Lipid Raft Fractionation—Cells were lysed in buffer containing 50 mM Tris-HCl, pH 8.0, 150 mM NaCl, 0.02% sodium azide, 400 nM microcystin-LR, 0.5 mM sodium vanadate, and 1% Nonidet P-40 with complete protease inhibitor mix (Sigma). Mouse brain homogenates were prepared from cortical tissue using a lysis buffer similar to that used for HEK293T cells except that Nonidet P-40 was replaced with 2% CHAPS, and the samples were sonicated on ice with 15–20 strokes. Antigens were detected by their corresponding primary and secondary antibodies followed by enhanced chemiluminescence (Pierce). Lipid raft fractionations were carried out as previously described (6).

Surface Biotinylation and Biotin Internalization Assays—For surface biotinylations, confluent cells in 6-well plates were washed 3 times in phosphate-buffered saline (PBS) and treated with 2.0 mg/ml sulfo-NHS-LC-biotin in PBS, pH 8.0, under gentle shaking for 1 h on ice. The cells were then washed 3 times in PBS and lysed in 1% Nonidet P-40 lysis buffer. Biotinylated proteins were isolated by pulldown with anti-biotin antibody together with anti-mouse-agarose beads. Biotin internalization assay was performed using previously described methods (15). Briefly, cells were grown on 6-well plate dishes and incubated twice for 20 min at 4 °C with 2 mg/ml non-membrane-permeating, cleavable biotin derivative sulfosuccinimidyl 2-(biotinamido)ethyl-1,3′-dithiopropionate (Pierce). Cells were then washed with cold PBS containing 0.1 M glycine followed by several washes with cold PBS. Cells were incubated with culture medium for 0, 5, 10, or 20 min at 37 °C to allow internalization of the labeled proteins. Internalization was stopped by rapid cooling on ice. To cleave biotin exposed at the cell surface, cells were incubated three times for 20 min at 4 °C with 50 mM 2-mercaptoethanesulfonic acid (Sigma) in 50 mM Tris-HCl, pH 8.7, 100 mM NaCl, and 2.5 mM $CaCl_2$. After thorough rinsing with PBS containing 20 mM Hepes, cells were lysed in 1% Nonidet P-40 buffer, and internalized biotinylated proteins were immunoprecipitated with anti-biotin antibody and subjected to immunoblotting for APP (CT15).

Primary Neuron Cultures—To prepare hippocampal primary neuronal cultures, hippocampi from both the hemispheres were separated and freed from meninges under a dissection microscope from newborn (P0) pups of APP transgenic mice, carrying both Swedish APP and presenilin-1 mutations (APPSwe, PSENdE9, 85 DboJ mice) (16). The hippocampi were washed 3× with Ca^{2+}/Mg^{2+}-free Hanks' balanced salt solution containing penicillin/streptomycin. The tissues were dissociated in 0.27% trypsin (in 10% Dulbecco's modified Eagle's medium/Hanks' balanced salt solution) by incubating at 37 °C for 30 min. Neurons were collected by centrifugation and resuspended in 10% Ham's F-12 medium (with penicillin/streptomycin). The neurons were further dissociated by triturating 20 times with a Pasteur pipette and passed through a cell strainer. After centrifugation, the neurons were resuspended in neurobasal medium containing 2% B-27 supplement, glutamine, pyruvate, and penicillin/streptomycin (50 units/ml penicillin, 50 υg/ml streptomycin) and plated on to a 24-well plate coated with 30 μg/ml poly-D-lysine in borate buffer (0.15 M, pH 8.4). A quarter of the growth medium was changed every 3 days.

Transient Transfections—Experiments involving transient transfections were performed using Lipofectamine 2000 (Invitrogen) and Opti-MEM I (Invitrogen). Equal amounts of empty vectors were included to keep the overall DNA quantity constant for all the experimental groups. A 19-nucleotide siRNA duplex targeting RanBP9, 5′-tcttatcaacaatacctgc-3′,

corresponding to human RanBP9 cDNA positions 868–886 relative to the first nucleotide of the start codon and scrambled control siRNA were synthesized and supplied in a 2′-deprotected, annealed, and desalted format from Dharmacon (Lafayette, CO). Either RanBP9-specific or single strand sense control siRNAs were transiently transfected at 50–100 nM final concentrations using Lipofectamine 2000 (Invitrogen) according to the manufacturer's instructions. Hippocampal neurons were grown for 7–10 days until a robust network of processes formed before transfections, and the neurons were similarly transfected with siRNA as previously described (17, 18). After 24 h of the first transfection (17, 18), a second transfection was performed to enhance the knock-down effect of the siRNA. Twenty-four hours after the second transfection, conditioned media were collected for sAPPβ and Aβ detection.

Aβ40 Enzyme-linked Immunosorbent Assay (ELISA)—Conditioned media were recovered, and debris was removed by centrifugation. Aβ in the conditioned medium was detected by sandwich ELISA. Aβ standards (Bachem) were dissolved in hexafluoroisopropanol at 1 mg/ml, sonicated, dried by blowing under nitrogen, resuspended at 2 mg/ml, sonicated, and dried under nitrogen. The dried Aβ was resuspended in DMSO, separated into aliquots, and frozen at −80 °C. Standards were loaded in duplicate at concentrations of 0, 12.5, 25, 50, 100, and 200 pmol/liter. Control media was also added to two wells in duplicate. Aβ was captured in the conditioned media with Ab9 antibody (epitope Aβ-(1–16)) coated at 10–50 μg/ml. The wells were then blocked overnight at 4 °C with blocking buffer (1% Block Ace, 0.05% NaN_3 in PBS, pH 7.4). After washing with PBS, the conditioned media containing soluble Aβ was loaded in duplicates at 100 μl/well without further dilution and incubated for 24 h at 4 °C. Aβ40 was detected with horseradish peroxidase-conjugated Ab13.1.1 (anti-Aβ35–40) antibody (1:1000 dilution of 1 mg/ml stock). Resulting antibody-bound Aβ was detected using 1:1 mixture of the tetramethyl benzidine developing solution (substrate + peroxide). Specificity of this ELISA for Aβ40 detection was tested using synthetic human Aβ (Bachem).

Statistical Analysis—All data were analyzed by Instat3 software using either Student's *t* test or one-way analysis of variance followed by a Kruskal-Wallis post hoc test. Data were expressed as the mean ± S.E. Differences were deemed significant at $p < 0.05$.

RESULTS

The C37 Region of LRP Binds to RanBP9 and Stabilizes the RanBP9·APP Complex—We previously showed that the C-terminal 37 amino acids of LRP tail (LRP-C37 sequence) interacted specifically with RanBP9 in the yeast 2-hybrid assay (7). Thus, we examined whether RanBP9/LRP interaction could be confirmed in mammalian cells. HEK293T cells were transiently transfected with a combination of FLAG-tagged RanBP9, LRP-L4 mini-receptor containing the fourth ligand binding domain, and APP751, and immunoprecipitations were carried out with anti-FLAG (M2) antibody. Western blots were carried out using CT15 for the detection of APP, 1704 for the detection of LRP, and M2 for the detection of FLAG-RanBP9. As expected, LRP was specifically detected in FLAG-RanBP9 (M2) immune complexes. Surprisingly, RanBP9 immune complexes also contained APP, which was robustly enhanced by co-expression of LRP-L4 (Fig. 1*A*). However, overexpression of LRP-L4 lacking the C37 region (ΔC37) failed to enhance the interaction between APP and RanBP9, indicating that LRP through its C37 domain stabilizes/promotes the APP·RanBP9 complex (Fig. 1*A*). In contrast, overexpression of APP did not further increase the amount of the RanBP9·LRP-L4 complex, indicating that LRP/RanBP9 interaction is not influenced by APP (Fig. 1*A*). Although the 1704 antibody against the C terminus of LRP does not detect ΔC37 (Fig. 1*A*), comparable levels of LRP-L4 and LRP-L4-ΔC37 expression were seen by HA antibody that detects both proteins (not shown). These data indicate that the C37 region of LRP functions to stabilize the interaction between RanBP9 and APP and suggest that LRP-ST and/or soluble LRP-C37 acts on APP trafficking and processing possibly by recruiting RanBP9 to APP-containing complexes.

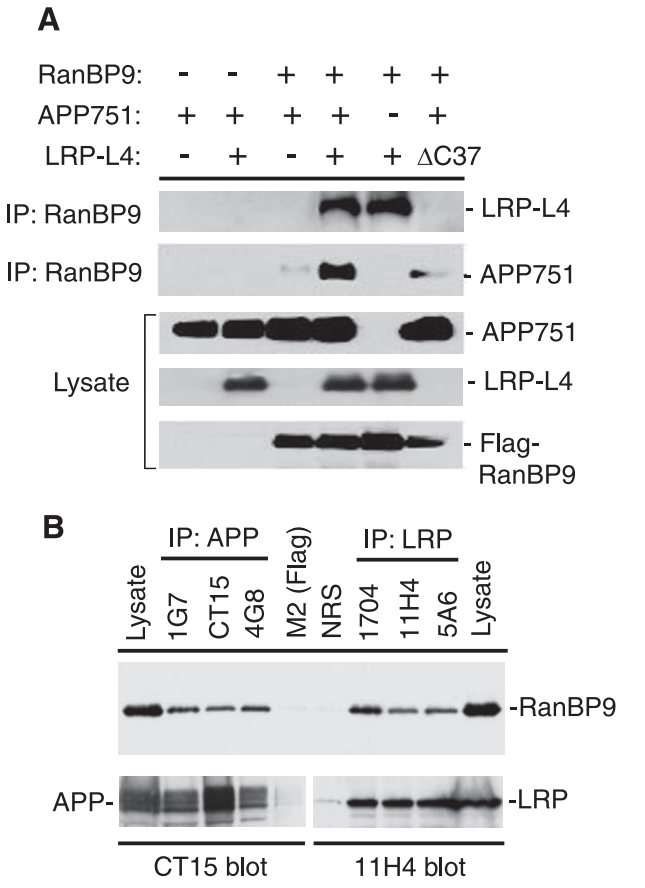

FIGURE 1. **RanBP9 physically associates with LRP and APP in mammalian cells and in brain.** *A*, RanBP9 binds both LRP and APP, and LRP promotes RanBP9·APP interaction. HEK293T cells were triple-transfected with combinations of FLAG-RanBP9, APP, and LRP-L4 or LRP-L4 lacking the C37 domain (*ΔC37*). Equal protein amounts were immunoprecipitated (*IP*) with anti-FLAG (M2, Sigma) antibody and immunoblotted for APP (CT15) and LRP (1704) (*upper two panels*). In the *lower three panels* equal amounts of lysates were immunoblotted for APP (CT15), LRP (1704), and FLAG-RanBP9 (M2). *B*, endogenous RanBP9 physically associates with endogenous APP and LRP *in vivo*. Wild type mouse brain homogenates were prepared from frontal cortical regions in 2% CHAPS buffer and subjected to immunoprecipitation with three APP and three LRP antibodies as indicated or normal rabbit serum and anti-FLAG (M2) antibody as negative controls. Endogenous RanBP9 was detected with anti-RanBP9 antibody. In the *bottom panels* immunoprecipitated proteins were immunoblotted for either APP (*CT15*) or LRP (*11H4*).

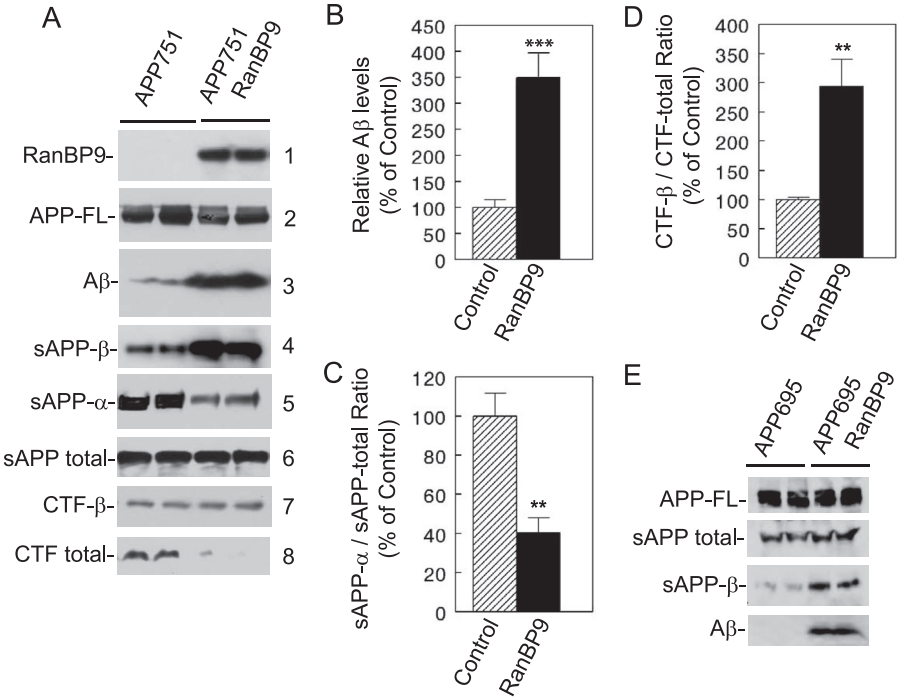

FIGURE 2. **RanBP9 robustly increases Aβ secretion by stimulating β-secretase processing of APP.** *A*, CHO-APP751 and CHO-APP751-RanBP9 stably transfected cells were plated at near confluency, and conditioned media were collected overnight. In the *first* and *second panels*, equal protein amounts of cell lysates were subjected to immunoblotting for FLAG-RanBP9 (*M2*) and APP (*CT15*). In the *third panel*, conditioned media were subjected to immunoprecipitation for Aβ (Ab9), and detection with mixed 6E10/82E1 antibodies. In the *fourth* to *sixth panels*, equal amounts of conditioned media were immunoblotted for sAPPα (6E10), sAPP total (63G), and sAPPβ (18957, IBL). In the *bottom two panels*, equal protein amounts of cell lysates were subjected to immunoblotting for APP CTF-β (6E10) and total APP CTF (CT15). *B*, densitometric quantitation of Aβ blots reveals an average ~3.5-fold increases in the Aβ levels in CHO-APP751-RanBP9-expressing cells compared with the parental CHO-APP751 cells. Mean ± S.E., $n = 6$ each; ***, $p < 0.001$ by Student's *t* test. *C*, densitometric quantitation reveals a significant decrease in sAPP-α relative to sAPP total in CHO-APP751-RanBP9 cells compared with parental CHO-APP751 cells (mean ± S.E., $n = 6$ each; **, $p < 0.01$ by Student's *t* test). *D*, densitometric quantitation reveals a significant increase in APP-CTF-β relative to total APP CTF in CHO-APP751-RanBP9 cells compared with parental CHO-APP751 cells (mean ± S.E., $n = 4$ each; **, $p < 0.01$ by Student's *t* test). *E*, RanBP9 increases β-secretase cleavage independent of the KPI domain. CHO-APP695 and CHO-APP695-RanBP9 stably transfected cells were plated at near confluency, and conditioned media were collected overnight. In the *first panel*, equal protein amounts of cell lysates were immunoblotted for APP (CT15). In the *second* and *third panels*, equal amounts of conditioned media were immunoblotted for sAPPβ (18957, IBL) and sAPP total (63G). In the *last panel*, equal amounts of conditioned medium were subjected to immunoprecipitation for Aβ (Ab9) and detection with mixed 6E10/82E1 antibodies.

Endogenous RanBP9 Interacts with LRP and APP in Brain—To determine whether endogenous RanBP9 normally interacts with LRP and APP *in vivo*, we next evaluated wild type mouse brains for these interactions. Mouse brain homogenates were prepared in 1% CHAPS buffer and immunoprecipitated with various APP and LRP antibodies. RanBP9 protein was detected by anti-RanBP9 monoclonal antibody (10). As shown in Fig. 1*B*, three APP antibodies used, 4G8, CT15, and 1G7, pulled down the endogenous RanBP9 protein. Similarly, three LRP antibodies used, 1704, 11H4, and 5A6, pulled down RanBP9 (Fig. 1*B*). In contrast, anti-FLAG antibody and normal rabbit serum used as negative controls failed to pull down any detectable RanBP9 (Fig. 1*B*). The amount of APP and LRP pulldown was similar from antibody to antibody and corresponded to similar amounts of RanBP9 pulldown. Taken together, this co-immunoprecipitation experiment from wild type mouse brain demonstrates that endogenous APP and LRP form complexes with endogenous RanBP9 *in vivo*.

RanBP9 Overexpression Robustly Increases BACE1 Processing of APP and Aβ Generation—Given that RanBP9 interacted specifically with both LRP and APP, we next tested the effects of RanBP9 overexpression on APP processing and Aβ production. In transiently transfected HEK293T cells, RanBP9 markedly enhanced the levels of Aβ in the conditioned medium (supplemental Fig. S1), similar to that seen with the soluble LRP-C37 polypeptide (7). To confirm these results in a different cellular system, we stably transfected FLAG-RanBP9 in CHO cells stably expressing APP751 (CHO-APP751). In these cells N-terminal-tagged FLAG-RanBP9 migrating at ~90 kDa was readily detected by the M2 anti-FLAG antibody (Fig. 2*A*). Stable overexpression of RanBP9 robustly elevated Aβ secretion into the conditioned medium of CHO-APP751 cells without changing the level of APP holoprotein (Fig. 2, *A* and *B*). Quantitation from multiple experiments ($n = 6$) showed that RanBP9-overexpressing CHO-APP751 cells secreted ~3.5 times more Aβ than parental CHO-APP751 control cells (Fig. 2*B*). Examination of the conditioned medium for sAPP demonstrated that RanBP9 markedly increased the secretion of sAPP-β and reduced sAPP-α without changing sAPP total (Fig. 2, *A* and *C*). Thus, the ratio of sAPP-α relative to sAPP total was reduced by an average of ~60% by RanBP9 (Fig. 2*C*). Surprisingly, overexpression of RanBP9 also led to a ~66% reduction in the steady state level of APP C-terminal fragments (CTFs) in CHO cells (Fig. 2*A*), suggesting a direct or indirect effect on APP-CTF turnover by γ-secretase or degradative processing. Despite the reduction in total APP-CTFs by RanBP9, APP-CTF-β remained relatively unchanged, thereby increasing the APP-CTF-β/APP-CTF total ratio by 3-fold (Fig. 2*D*). Taken together, these data support the notion that RanBP9 preferentially promotes β-secretase processing of APP at the expense of α-secretase cleavage in CHO-APP751 cells.

As LRP is capable of physically associating with both the cytoplasmic tail and KPI domains of APP, we next tested whether the effects of RanBP9 in promoting β-secretase processing of APP was unique to APP751, which contains the KPI domain, or also seen in APP695, which lacks the KPI domain. Thus, we stably transfected CHO cells expressing APP695 with RanBP9 and measured the amount of sAPP total, sAPP-β, and Aβ in the conditioned medium. As seen in CHO- APP751 cells,

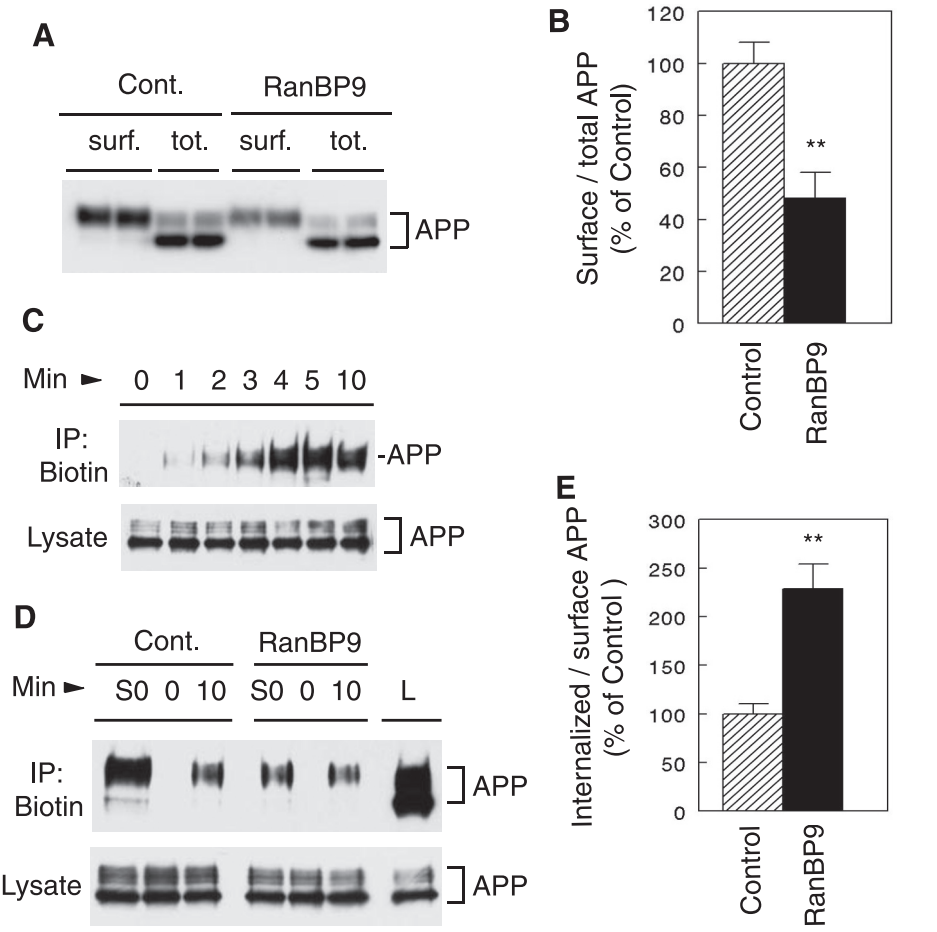

FIGURE 3. **RanBP9 overexpression reduces cell surface APP and promotes APP internalization.** *A*, CHO-APP751 and CHO-APP751-RanBP9 stable cells were surface-biotinylated on ice, and lysates were immunoprecipitated with anti-biotin antibody followed by detection of APP by CT15 antibody. A representative experiment is shown. *B*, densitometric quantification using image J software reveals a ~52% reduction of surface levels of APP relative to total APP in the presence of RanBP9 (t = 3.94, $p = 0.0028$ (**), df = 10). *Error bars* represent S.E. *C*, to determine the kinetics of APP internalization, CHO-APP751 cells surface-biotinylated with cleavable biotin on ice and returned to 37 °C for the indicated times to allow internalization of labeled proteins. The remaining cell surface biotin was removed by 2-mercaptoethanesulfonic acid, and equal amounts of cell lysates were immunoprecipitated (*IP*) with anti-biotin antibody (internalized proteins) followed by immunodetection for APP (CT15, *upper panel*). Note that the non-internalized controls (0 min) show no internalization, indicating that removal of surface biotin is complete and internalization peaks at 5–10 min. In the *lower panel*, equal amounts of cell lysates were directly immunoblotted for APP (CT15). *D*, a representative biotin surface labeling and internalization experiment from control CHO-APP751 and CHO-APP751-RanBP9 cells according procedures in *C*. *S0* indicates total surface labeling before removal of surface biotin, whereas *0* and *10* min indicate time points of internalization. In the *bottom panel* and *L* in the *top panel*, equal lysate volumes were subjected to direct immunoblotting for APP (CT15). *E*, quantitative measurement of internalized APP after 10 min normalized to surface APP at time zero determined in the same experiments (t = 5.006, $p = 0.0007$ (**), df = 10). *Error bars* represent S.E. Note the significantly increased rate of APP internalization relative to surface APP in CHO-APP751-RanBP9 cells compared with parental CHO-APP751 cells.

we found a similar robust increase in secretion of sAPP-β and Aβ without significantly altering the total amounts of cellular or secreted APP (Fig. 2*E*). Thus, the ability of RanBP9 to stimulate APP β-secretase processing appears to be largely independent of the KPI/LRP interaction.

Unlike wild type APP that requires endocytosis for efficient β-secretase cleavage (19, 20), the FAD Swedish APP mutation is efficiently cleaved by BACE1 en route to the cell surface in the secretory pathway (21–23). To determine whether RanBP9 can also enhance β-secretase processing of Swedish APP, we stably transfected N2a cells expressing Swedish APP695 with FLAG-RanBP9. Using an antibody against the β-secretase cleavage site of Swedish sAPP (6A1), we found that RanBP9 indeed robustly increased sAPPβ secretion by ~3-fold without altering the level of cellular APP (Supplemental Fig. S2). Thus, these data taken together demonstrate that RanBP9 promotes β-secretase activity in both non-neuronal and neuronal cells from wild type and Swedish APP.

RanBP9 Overexpression Reduces Cell Surface APP and Accelerates APP Internalization—Our observation that RanBP9 robustly enhanced BACE1 cleavage of both wild type and Swedish APP suggested that RanBP9 could exert its pro-amyloidogenic activity in both secretory and endocytic processing pathways. To determine whether RanBP9 affects the endocytosis of APP, we first measured the level of APP on the cell surface. The cell surface of CHO-APP751 and CHO-APP751-FLAG-RanBP9 cells were biotinylated on ice, and lysates were subjected to immunoprecipitations with anti-biotin antibody to pull down biotinylated surface proteins. As expected, fully mature and slower migrating APP was preferentially biotinylated on the surface (Fig. 3*A*). Relative to total APP in cell lysates, RanBP9 overexpression significantly reduced the level of surface APP by 52% compared with parental control cells (Fig. 3*B*; $p = 0.0028$, t = 3.94, df = 10).

The decrease in surface APP can result from accelerated internalization of APP, an event thought to be critical for Aβ generation from wild type APP (19, 20). Thus, increased APP endocytosis could explain the increased Aβ production and reduced surface APP by RanBP9. Alternatively, increased β-secretase processing of APP en route to the cell surface (secretory pathway) could result in decreased APP on the cell surface, as precisely seen in the APP Swedish double mutation (21–23). Thus, we measured the internalization of APP in CHO-APP751 and CHO-APP751-RanBP9 cells using biotin internalization assay (15). Cells were surface-biotinylated with a cleavable biotin derivative on ice and returned to the 37 °C incubator for 0, 1, 2, 3, 4, 5, or 10 min for internalization to proceed. Then non-internalized surface biotin was completely removed, and lysates were subjected to immunoprecipitation for biotin and detection of biotinylated and internalized APP. As shown in Fig. 3*C*, there was little to no biotinylated APP at time 0, indicating that the removal of surface biotin was complete. As the amount of

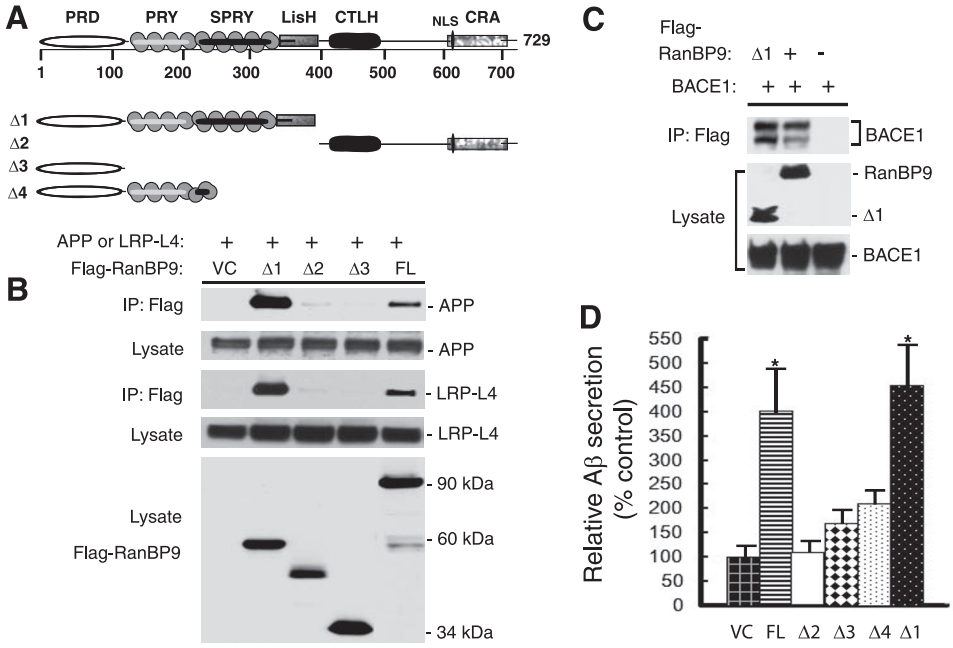

FIGURE 4. **SPRY-LisH domains of RanBP9 are sufficient to strongly interact with LRP, APP, and BACE1 and increase Aβ generation.** *A*, schematic of domain organization of RanBP9 and FLAG-tagged deletion constructs: *Δ1* (residues 1–392), *Δ2*, (residues 408–729), *Δ3* (residues 1–107), and *Δ4* (residues 1–254). *B*, SPRY-LisH domains bind strongly to LRP and APP. HEK293T cells were transiently co-transfected with APP or LRP-L4 together with vector control (*VC*), FLAG-tagged RanBP9, Δ1, Δ2, or Δ3 deletion mutants. Equal protein amounts were subjected to immunoprecipitation (*IP*) for FLAG-RanBP9 variants (M2) and immunoblotted for APP (CT15) or LRP (1704). Equal protein amounts from lysates were also directly immunoblotted for APP (CT15), LRP (1704), and FLAG (M2). Note that transient transfection of RanBP9-FL also yields an N-terminal 60-kDa fragment (N60), which comigrates with the RanBP9-Δ1 mutant (residues 1–392). *C*, BACE1 coimmunoprecipitates with RanBP9 and RanBP9-Δ1. In the *upper panel*, HEK293T cells were co-transfected with GFP-BACE1 and FLAG-RanBP9-FL or FLAG-RanBP9-Δ1, and equal protein amounts were immunoprecipitated for FLAG (M2) and immunoblotted for BACE1 (B279). In the *lower two panels*, equal protein amounts of cell lysates were directly immunoblotted for RanBP9 (M2) and BACE1 (B279). *D*, SPRY-LisH domains are sufficient to robustly increase Aβ secretion. Conditioned medium from CHO-APP-751 cells stably expressing full-length or various deletion mutants of RanBP9 were immunoprecipitated for Aβ and quantitated by densitometry using Image J. The graph shows the means ± S.E. normalized to vector control. $n = 4$ each group; *, $p < 0.01$ by one-way analysis of variance followed by post hoc Kruskal-Wallis test.

biotinylated internalized APP began to peak at 5–10 min, we chose the 10-min time period to quantitate APP internalization relative to surface APP (Fig. 3, *D* and *E*). Quantitation from multiple internalization experiments revealed that RanBP9 led to a ~2.3-fold increase in APP internalization relative to the amount of surface APP determined in each experiment (Fig. 3, *D* and *E*; $p = 0.0007$, $t = 5.006$, $df = 10$). This indicates that increased internalization of APP at least in part accounts for the reduction in surface APP and the increase in β-secretase processing and Aβ generation in these cells.

SPRY-LisH Domains of RanBP9 Interact with APP, LRP, and BACE1 and Promote Aβ Generation—RanBP9 contains four putative conserved domains, B30.2/SPRY (SPla and the ryanodine receptor), LisH (Lissencephaly type-1 like homology), CTLH (C-terminal to LisH), and CRA (CT11-RanBP9). The B30.2/SPRY domain is known to be involved in various protein-protein interactions and LisH/CTLH domain in dimerization and or binding to microtubules. To identify the critical region within RanBP9 required for the interaction with APP and LRP, we engineered various deletion mutants of N-terminally FLAG tagged RanBP9 (Fig. 4*A*). RanBP9 variants were then co-transfected with either APP or LRP-L4 in HEK293T cells, and lysates were subjected to immunoprecipitations with anti-FLAG antibody (M2). As expected, APP co-immunoprecipitated with RanBP9, whereas the vector control (*VC*) failed to pull down APP (Fig. 5*B*). The Δ1 C-terminal deletion mutant (expressing residues from 1–392), which retains the proline-rich domain (PRD), SPRY (SPIa and the ryanodine receptor), and LisH domains but not CTLH and CRA domains, strongly interacted with APP (Fig. 4*B*). Surprisingly, the interaction between APP and the ~60-kDa Δ1 deletion mutant was much stronger than the full-length RanBP9 (Fig. 4*B*). In contrast, the Δ2 deletion mutant (residues 408–729), which contains the CTLH and CRA domains but not SPRY or LisH domains, failed to interact with APP (Fig. 4*B*). Similarly, the Δ3 deletion mutant that contains residues 1–107 also failed to co-precipitate with APP (Fig. 4*B*), indicating that residues from 108 to 392 comprising SPRY and LisH domains mediate the interaction with APP. The pattern of interactions between RanBP9 variants with LRP-L4 was essentially identical to APP, with the Δ1 mutant interacting much more strongly to LRP than full-length RanBP9 and Δ2 and Δ3 failing to pull down LRP-L4 (Fig. 4*B*). Because RanBP9 robustly stimulated β-secretase processing of APP, we next tested whether BACE1 itself could form a complex with RanBP9. Indeed, a recent study isolated RanBP9 as one of several potential BACE1-interacting proteins in a yeast two-hybrid screen using the BACE1 cytoplasmic tail as bait (24). HEK293T cells were transiently transfected with a combination of APP and/or GFP-BACE1 together with FLAG-RanBP9-FL or FLAG-RanBP9-Δ1, and cell lysates were subjected to immunoprecipitation with anti-FLAG M2 antibody. Indeed, BACE1 robustly co-precipitated with RanBP9, and this interaction was even more robust with the RanBP9-Δ1 mutant (Fig. 4*C*), similar to that seen with LRP and APP. These results demonstrate that the SPRY-LisH domains of RanBP9 form complexes with APP, LRP, and BACE1.

To identify which regions of RanBP9 that are necessary and/or sufficient to enhance Aβ generation, we stably transfected CHO-APP751 cells with RanBP9 deletion variants (Δ1–Δ4). Measurement of Aβ levels from conditioned media demonstrated that the Δ2 mutant lacking the SPRY and LisH domains completely failed to enhance Aβ release (Fig. 4*D*). Therefore, the CTLH and CRA domains alone do not influence Aβ levels. The Δ3 mutant containing the PRD and Δ4 mutant containing the PRD and part of the SPRY domain marginally elevated Aβ levels but did not differ significantly from vector

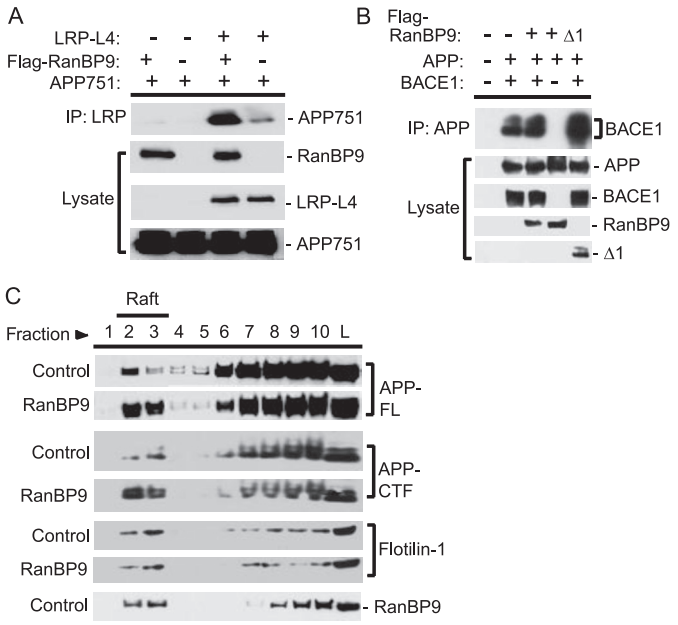

FIGURE 5. **RanBP9 promotes the physical association of APP with LRP and BACE1 and facilitates APP association with buoyant detergent-resistant raft fractions.** *A*, RanBP9 promotes the physical association of APP with LRP. In the *upper panel*, HEK293T cells were transfected with combinations of LRP-L4, APP, and FLAG-RanBP9 constructs, and equal protein amounts were immunoprecipitated (*IP*) for LRP-L4 (11H4) and immunoblotted for APP (CT15). In the *lower three panels*, equal protein amounts of cell lysates were directly immunoblotted for RanBP9 (M2), LRP-L4 (1704), and APP (CT15). *B*, RanBP9 promotes the physical association of APP with BACE1 in HEK293T cells. In the *upper panel*, HEK293T cells were co-transfected with combinations of GFP-BACE1, APP, and FLAG-RanBP9-FL or FLAG-RanBP9-Δ1, and equal protein amounts were immunoprecipitated for APP (IG7) and immunoblotted for BACE1 (B279). In the *lower four panels*, equal protein amounts of cell lysates were directly immunoblotted for APP (CT15), BACE1 (B279), and RanBP9 (M2). *C*, RanBP9 promotes the association of APP with lipid rafts. CHO-APP751 and CHOAPP751-RanBP9 stable cells were lysed in CHAPS buffer and subjected to discontinuous sucrose density gradient ultracentrifugation fractionation as previously reported (6). Equal volumes from each fraction were subjected to immunoblotting for full-length (*FL*) APP, CTFs, flotillin, and endogenous RanBP9. *L* indicates total lysate before fractionation.

control cells (Fig. 4*D*). In contrast, the Δ1 mutant (residues 1–392) containing the PRD, SPRY, and LisH domains enhanced Aβ production by ~4.5-fold over vector control (Fig. 4*D*). Interestingly, the Δ1 mutant increased Aβ levels somewhat more than full-length RanBP9, suggesting potential functional significance of increased binding of the Δ1 mutant with LRP and APP. Therefore, the capacity of RanBP9 via its SPRY and LisH domains to interact with APP, LRP, and BACE1 correlates with enhanced Aβ generation.

RanBP9 Stabilizes APP Complexes with LRP and BACE1 and Increases APP Association with Lipid Rafts—Previous studies have suggested that RanBP9 functions as a scaffolding protein capable of interacting with various membrane and cytosolic proteins (8–11). The formation of RanBP9 complexes with APP, LRP, and BACE1 may occur independently of each other. Alternatively, RanBP9 may be capable of scaffolding and stabilizing APP complexes with LRP and/or BACE1. We previously showed that knockdown of endogenous LRP dramatically reduces and overexpression of LRP soluble tail enhances Aβ generation (6). In addition, LRP soluble tail promoted the interaction between APP and BACE1 (6). Thus, stabilization of APP·LRP and/or APP·BACE1 complexes by scaffolding their cytoplasmic tails via RanBP9 is predicted to enhance Aβ generation. HEK293T cells were transfected with a combination of LRP, APP, and/or RanBP9, and lysates were subjected to immunoprecipitation with the 11H4 anti-LRP antibody. As expected, APP specifically coimmunoprecipitated with LRP (Fig. 5*A*). However, the amount of LRP·APP complex was robustly enhanced when RanBP9 was coexpressed with LRP and APP (Fig. 5*A*). Thus, LRP not only enhances APP·RanBP9 complex (Fig. 1*A*), but RanBP9 also reinforces the APP·LRP complex. In addition, HEK293T cells were also transiently transfected with a combination of BACE1, APP, and/or RanBP9, and lysates were subjected to immunoprecipitation with the IG7 anti-APP antibody. Similar to that seen with the APP·LRP complex, RanBP9 also increased the amount of the APP·BACE1 complex, an effect that was strongly further enhanced by the RanBP9-Δ1 mutant (Fig. 5*B*). Likewise, a similar stabilization of the APP·BACE1 complex by RanBP9 overexpression was also observed in transiently transfected N2a cells (supplemental Fig. S3). These data taken together indicate that RanBP9 positively regulates the physical association of APP cytoplasmic tail with the tails of LRP and BACE1 presumably via a scaffolding mechanism, both of which augment β-secretase processing of APP.

The proteolytic processing of APP to generate Aβ is thought to take place in cholesterol-rich buoyant detergent-resistant membranes (*i.e.* lipid rafts). Given that BACE1 and LRP are both raft-associated proteins and oligomerization of membrane proteins generally increases their affinity for rafts (6, 25–27), we next tested whether RanBP9 also promotes the association of APP with detergent-resistant membranes. CHAPS extracts from control CHO-APP751 and CHO-APP751-RanBP9 stable cells were analyzed by discontinuous sucrose density gradient fractionation as described previously (6). We examined the distribution pattern of APP, CTFs, RanBP9, and also flotillin-1 as a raft marker across sucrose gradient fractions 1–10. As expected, flotillin-1 was enriched in lipid raft fractions 2 and 3, representing the interface between 5 and 35% sucrose layers in both cell lines, indicating that RanBP9 does not affect its distribution (Fig. 5*C*). Similar to our previous observations, immunoblotting with CT15 antibody detected full-length APP in all but the first fraction, with a small amount in raft fractions. Remarkably, overexpression of RanBP9 altered the relative distribution of full-length APP as well as APP CTFs from heavier fractions to lipid raft fractions 2 and 3 (Fig. 5*C*). Careful observation also revealed that RanBP9 overexpression increased CTF-β relative to the faster migrating CTF-α in the raft fractions (Fig. 5*C*). Importantly, endogenous RanBP9 was also enriched in raft fraction 2 and 3, consistent with its role in promoting APP association with rafts (Fig. 5*C*). Thus, these data indicate that RanBP9 via its interactions with APP, LRP, and BACE1 promotes β-secretase processing and association of APP with detergent-resistant membrane rafts.

Endogenous RanBP9 Is Pivotal for Aβ Production—Thus far we showed that exogenous RanBP9 robustly enhanced β-secretase processing of APP and Aβ production. To determine whether endogenous RanBP9 normally contributes to Aβ generation, we used siRNA duplexes to silence the expression of endogenous RanBP9 in CHO-APP751 cells. Transient transfections of the RanBP9 siRNA reduced the expression of endoge-

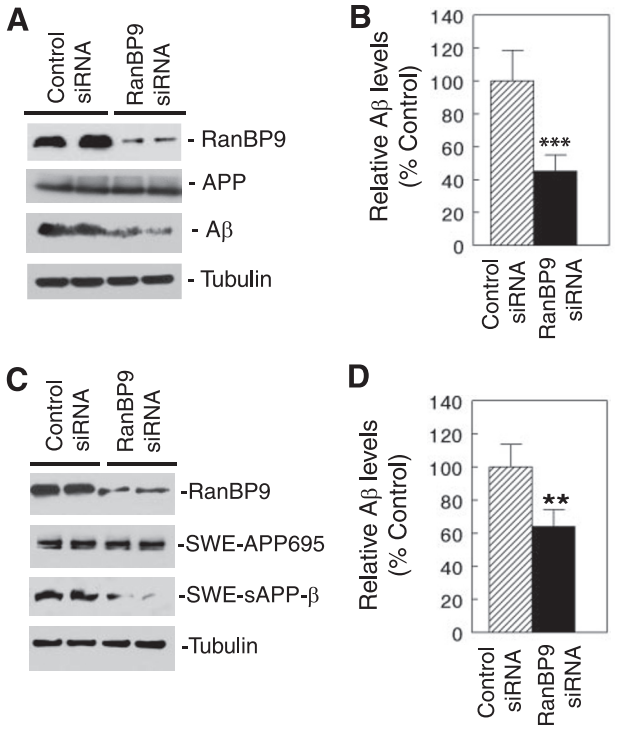

FIGURE 6. **Endogenous RanBP9 is pivotal for Aβ secretion in CHO cells and primary neurons.** *A*, CHO-APP751 stable cells were transiently transfected either with control sense siRNA or RanBP9-specific siRNA twice over a 48-h interval. After 24 h of the second transfection, lysates were immunoblotted for RanBP9 (anti-RanBP9), APP (CT15), and tubulin (anti-tubulin). The conditioned medium was immunoprecipitated with Ab9 antibody and immunoblotted for Aβ (6E10/82E1 mix). *B*, Aβ levels quantified from control siRNA and RanBP9 siRNA-transfected CHO-APP751 cells by image J software showed highly significant reduction by RanBP9 siRNA (Student's *t* test, mean $\pm$ S.E., $n = 4$ each; ***, $p < 0.001$). *C*, primary hippocampal neurons were grown for 7–10 days until a robust network of processes formed and then were transiently transfected with control sense or RanBP9 siRNA duplexes. After two rounds of transfection, equal protein amounts of cell lysates were immunoblotted for total APP (CT15), RanBP9 (anti-RanBP9), and tubulin. Equal amounts of overnight-conditioned media were directly immunoblotted for SWE-sAPPβ (6A1; *upper panel*). A representative experiment is shown. *D*, conditioned media from control and RanBP9 siRNA-transfected primary hippocampal neurons were subjected to ELISA for Aβ40. The graph shows the means and S.E. from four independent experiments normalized to control siRNA, illustrating a ~36% reduction in Aβ40 secretion by RanBP9 siRNA (*t* test; **, $p < 0.01$).

nous RanBP9 by about ~80% compared with the transfection of sense control oligo but did not alter APP or tubulin levels (Fig. 6*A*). At the same time RanBP9 siRNA reduced the secretion of Aβ by close to ~60% (Fig. 6, *A* and *B*), demonstrating that endogenous RanBP9 is an essential regulatory factor in Aβ generation. To confirm that RanBP9 is also a critical regulator of APP processing in neurons, we cultured primary neurons from the hippocampus of newborn (P0) APP/PS1 transgenic mice bearing the APP Swedish and PS1 ΔE9 mutations (16). Neurons were grown for 7–10 days until a robust network of processes formed and then were transiently transfected with control sense or RanBP9 siRNA duplexes. After 2 rounds of transfections, the conditioned medium was collected for detection of sAPPβ by immunoblotting and Aβ40 by ELISA. Lysates were collected for detection of endogenous RanBP9, APP, and tubulin. Double transfections of RanBP9 siRNA reduced endogenous RanBP9 levels by an average of ~50% without altering the levels of endogenous full-length APP or tubulin (Fig. 6*C*). Neither control nor RanBP9 siRNA transfections resulted in gross alterations in neuronal morphology or toxicity (supplemental Fig. S4). Examination of the conditioned media showed a consistent reduction in sAPP-β secretion by RanBP9 knockdown (Fig. 6*C*). Consistent with these findings, RanBP9 knockdown significantly reduced Aβ40 secretion by an average of ~36% from 4 independent experiments (Fig. 6*D*). These results taken together demonstrate that endogenous RanBP9 plays a critical role in Aβ production in both non-neuronal and neuronal cells.

DISCUSSION

The proteolytic processing of APP to generate Aβ is a primary event in the pathogenesis of AD. Therefore, understanding the manner in which APP and the secretases are brought together is critical for designing therapeutic strategies for AD. Previous studies have shown that the Reticulon family of proteins binds to BACE1 and prevents its access to APP, thereby reducing β-secretase processing and Aβ generation (28, 29). However, the molecular mechanisms by which APP and BACE1 comes in close proximity to each other in transient or stable complexes is essentially unknown. In this study we demonstrated that RanBP9 strongly enhanced BACE1 cleavage of APP and Aβ generation in non-neuronal (HEK293T and CHO cells) and neuronal (N2a) cell lines as well as in primary neurons. This increased β-secretase processing of APP by RanBP9 was not dependent on the KPI domain of APP or the Swedish APP mutation. In wild type APP-expressing cells, RanBP9 reduced surface APP and enhanced APP internalization, consistent with a role of RanBP9 in promoting endocytic processing of APP. We also presented evidence that RanBP9 increased BACE1 processing of APP and Aβ generation by scaffolding interactions among APP, LRP, and BACE1. Specifically, LRP via its C37 domain not only interacted with RanBP9 but also promoted the interaction between APP and RanBP9. Conversely, RanBP9 also stabilized APP·LRP complexes, thereby mutually reinforcing the RanBP9·LRP·APP complex. In addition, RanBP9 also formed complexes with BACE1 and promoted the physical association of APP complexes with BACE1, suggesting that RanBP9 serves to bridge and/or stabilize these multiprotein interactions via a scaffolding mechanism. Like LRP and BACE1 (6, 27), we found that RanBP9 is also enriched in rafts, consistent with its role in promoting the localization of APP to raft microdomains where Aβ generation occurs (27, 30). Finally, endogenous RanBP9 was required for the normal generation of Aβ in both CHO cells and primary neurons, demonstrating its normal physiological activity in APP processing.

RanBP9 and LRP-ST similarly increased Aβ, sAPP-β, and APP localization to lipid rafts and stabilized APP·BACE1 interactions (5–7). In view of these similarities as binding partners, we interpret these data to indicate that LRP-ST in part promotes the amyloidogenic processing of APP by recruiting or mobilizing endogenous RanBP9 to APP complexes. Although it is likely that endogenous full-length LRP also recruits RanBP9 to APP complexes, it is notable that the extracellular ligand binding domains II and IV of LRP also interact with the extracellular KPI domain of APP, and the loss of the cytoplasmic tail in LRP-L4 mini-receptor does not abrogate its interaction with

APP770 (31). Thus, it is likely that endogenous LRP affects APP processing via both cytoplasmic and extracellular domains.

Unlike wild type APP, which requires internalization from the cell surface to generate Aβ (19, 20), FAD Swedish APP is a superior substrate for BACE1 and is mostly cleaved en route to the cell surface in the secretory pathway (21–23, 32). Therefore, the ability of RanBP9 to enhance BACE1 cleavage of APP and Aβ generation in both wild type and Swedish APP from overexpression and siRNA studies indicates that RanBP9 acts to facilitate APP/BACE1 interaction and Aβ generation in both secretory and endocytic vesicles. The observation that RanBP9 reduced surface APP and accelerated APP internalization constitutes direct evidence that RanBP9 at least in part promotes BACE1 cleavage of APP via the endocytic pathway. Similarly, it has been shown that LRP promotes APP internalization and Aβ generation (3). Whether LRP recruits RanBP9 and/or *vice versa* to accelerate APP endocytosis is an important question to be addressed.

LRP, APP, and BACE1 specifically interacted with the SPRY-LisH domains of RanBP9. The B30.2/SPRY domain of RanBP9 contains a less-conserved 64-residue region called PRY domain (residues 147–211) followed by the highly conserved core SPRY domain (residues 212–333). This structural organization may be useful for permitting the simultaneous binding of 2 or more proteins of differing structure or sequence motif. The RanBP9-Δ4 mutant containing the PRY domain and part of the core SPRY domain was capable of interacting with LRP (not shown) but only marginally increased Aβ production, indicating the requirement of the core SPRY and LisH domains for full activity. LisH domains are found in a variety of proteins, the most famous being lissencephaly-1, a gene mutated in the human neuronal migration disorder lissencephaly (33). Interestingly, LisH domain in lissencephaly-1 is involved in the dimerization of the protein, and LisH domains in other proteins have been shown to promote homo- and hetero-dimerization and oligomerization of proteins (34, 35). Thus, it is likely that RanBP9 exists as dimers or oligomers, lending to the notion that RanBP9 may be able to scaffold multiple APP, LRP, and BACE1 molecules simultaneously. Indeed, it has been shown that RanBP9 exists in large multiprotein complexes of greater than 670 kDa (36), suggesting that 2 or more RanBP9 molecules may be present in the complex. The N-terminal PRD (*i.e.* RanBP9-Δ3) was neither sufficient to interact with LRP and APP nor significantly enhance Aβ generation. However, it is possible that PRD together with B30.2/SPRY and LisH domains play a role in the scaffolding mechanism (37). Because the PRD of Scramblase-1 interacts with BACE1 (38), the PRD of RanBP9 may also be involved in binding to BACE1. It has been shown that the PRD of RanBP9 is critical for recruiting a signaling component of the Ras-ERK pathway, Sos, upon binding to the hepatocyte growth factor receptor, Met, via its SPRY domain (9).

This study demonstrated that RanBP9 could potentially be a promising therapeutic target for AD as siRNA knockdown studies reduced β-secretase cleavage and Aβ levels. A novel therapeutic strategy might be to reduce RanBP9 levels and/or specifically disrupt its interactions with APP, LRP, and/or BACE1. This would be predicted to diminish Aβ generation without directly altering BACE1 enzymatic activity, which controls the myelination of the central nervous system and peripheral axons (39, 40). RanBP9 has been shown to exert pro-apoptotic effects in conjunction with the p73 tumor suppressor protein (41) and cooperate with Plexin-A to strongly inhibit axonal outgrowth *in vitro* and *in vivo* (11). Thus, reducing RanBP9 levels and/or activity may also lead to neuroprotection in addition to its effects on Aβ generation. Further studies on the biology of RanBP9 in the adult brain and body are, therefore, warranted.

Acknowledgments—We thank Dr. Sang-Ohk-Shim of Yale University for the pFLAG-RanBP9 construct, Dr. Marie-France-Langlois of University of Sherbrook for the pcDNA3-RanBP9 construct, Dr. Marilyn Farquhar of the University of California, San Diego for the pLNCX-LRP-L4 construct, and Dr. R. Yan of the Cleveland Clinic for the B279 antibody against BACE1.

REFERENCES

1. De Strooper, B., and Annaert, W. (2000) *J. Cell Sci.* **113,** 1857–1870
2. Herz, J., and Strickland, D. K. (2001) *J. Clin. Investig.* **108,** 779–784
3. Pietrzik, C. U., Busse, T., Merriam, D. E., Weggen, S., and Koo, E. H. (2002) *EMBO J.* **21,** 5691–5700
4. Ulery, P. G., Beers, J., Mikhailenko, I., Tanzi, R. E., Rebeck, G. W., Hyman, B. T., and Strickland, D. K. (2000) *J. Biol. Chem.* **275,** 7410–7415
5. Yoon, I. S., Pietrzik, C. U., Kang, D. E., and Koo, E. H. (2005) *J. Biol. Chem.* **280,** 20140–20147
6. Yoon, I. S., Chen, E., Busse, T., Repetto, E., Lakshmana, M. K., Koo, E. H., and Kang, D. E. (2007) *FASEB J.* **21,** 2742–2752
7. Lakshmana, M. K., Chen, E., Yoon, I. S., and Kang, D. E. (2008) *J. Cell Mol. Med.* **12,** 2665–2674
8. Hafizi, S., Gustafsson, A., Stenhoff, J., and Dahlback, B. (2005) *Int. J. Biochem. Cell Biol.* **37,** 2344–2356
9. Wang, D., Li, Z., Messing, E. M., and Wu, G. (2002) *J. Biol. Chem.* **277,** 36216–36222
10. Denti, S., Sirri, A., Cheli, A., Rogge, L., Innamorati, G., Putignano, S., Fabbri, M., Pardi, R., and Bianchi, E. (2004) *J. Biol. Chem.* **279,** 13027–13034
11. Togashi, H., Schmidt, E. F., and Strittmatter, S. M. (2006) *J. Neurosci.* **26,** 4961–4969
12. Dansereau, D. A., and Lasko, P. (2008) *J. Cell Biol.* **182,** 963–977
13. Valiyaveettil, M., Bentley, A. A., Gursahaney, P., Hussien, R., Chakravarti, R., Kureishy, N., Prag, S., and Adams, J. C. (2008) *J. Cell Biol.* **182,** 727–739
14. Mucke, L., Masliah, E., Yu, G. Q., Mallory, M., Rockenstein, E. M., Tatsuno, G., Hu, K., Kholodenko, D., Johnson-Wood, K., and McConlogue, L. (2000) *J. Neurosci.* **20,** 4050–4058
15. Graeve, L., Drickamer, K., and Rodriguez-Boulan, E. (1989) *J. Cell Biol.* **109,** 2809–2816
16. Jankowsky, J. L., Fadale, D. J., Anderson, J., Xu, G. M., Gonzales, V., Jenkins, N. A., Copeland, N. G., Lee, M. K., Younkin, L. H., Wagner, S. L., Younkin, S. G., and Borchelt, D. R. (2004) *Hum. Mol. Genet.* **13,** 159–170
17. Dalby, B., Cates, S., Harris, A., Ohki, E. C., Tilkins, M. L., Price, P. J., and Ciccarone, V. C. (2004) *Methods* **33,** 95–103
18. Tonges, L., Lingor, P., Egle, R., Dietz, G. P., Fahr, A., and Bahr, M. (2006) *RNA* **12,** 1431–1438
19. Koo, E. H., and Squazzo, S. L. (1994) *J. Biol. Chem.* **269,** 17386–17389
20. Perez, R. G., Soriano, S., Hayes, J. D., Ostaszewski, B., Xia, W., Selkoe, D. J., Chen, X., Stokin, G. B., and Koo, E. H. (1999) *J. Biol. Chem.* **274,** 18851–18856
21. Thinakaran, G., Teplow, D. B., Siman, R., Greenberg, B., and Sisodia, S. S. (1996) *J. Biol. Chem.* **271,** 9390–9397
22. Haass, C., Lemere, C. A., Capell, A., Citron, M., Seubert, P., Schenk, D., Lannfelt, L., and Selkoe, D. J. (1995) *Nat. Med.* **1,** 1291–1296

23. Perez, R. G., Squazzo, S. L., and Koo, E. H. (1996) *J. Biol. Chem.* **271,** 9100–9107
24. Wickham, L., Benjannet, S., Marcinkiewicz, E., Chretien, M., and Seidah, N. G. (2005) *J. Neurochem.* **92,** 93–102
25. Ehehalt, R., Keller, P., Haass, C., Thiele, C., and Simons, K. (2003) *J. Cell Biol.* **160,** 113–123
26. Harder, T., Scheiffele, P., Verkade, P., and Simons, K. (1998) *J. Cell Biol.* **141,** 929–942
27. Riddell, D. R., Christie, G., Hussain, I., and Dingwall, C. (2001) *Curr. Biol.* **11,** 1288–1293
28. He, W., Lu, Y., Qahwash, I., Hu, X. Y., Chang, A., and Yan, R. (2004) *Nat. Med.* **10,** 959–965
29. Murayama, K. S., Kametani, F., Saito, S., Kume, H., Akiyama, H., and Araki, W. (2006) *Eur. J. Neurosci.* **24,** 1237–1244
30. Cordy, J. M., Hussain, I., Dingwall, C., Hooper, N. M., and Turner, A. J. (2003) *Proc. Natl. Acad. Sci. U. S. A.* **100,** 11735–11740
31. Cam, J. A., Zerbinatti, C. V., Li, Y., and Bu, G. (2005) *J. Biol. Chem.* **280,** 15464–15470
32. Vassar, R., Bennett, B. D., Babu-Khan, S., Kahn, S., Mendiaz, E. A., Denis, P., Teplow, D. B., Ross, S., Amarante, P., Loeloff, R., Luo, Y., Fisher, S., Fuller, J., Edenson, S., Lile, J., Jarosinski, M. A., Biere, A. L., Curran, E., Burgess, T., Louis, J. C., Collins, F., Treanor, J., Rogers, G., and Citron, M. (1999) *Science* **286,** 735–741
33. Reiner, O., Sapoznik, S., and Sapir, T. (2006) *Neuromolecular Med.* **8,** 547–565
34. Gerlitz, G., Darhin, E., Giorgio, G., Franco, B., and Reiner, O. (2005) *Cell Cycle* **4,** 1632–1640
35. Mateja, A., Cierpicki, T., Paduch, M., Derewenda, Z. S., and Otlewski, J. (2006) *J. Mol. Biol.* **357,** 621–631
36. Nishitani, H., Hirose, E., Uchimura, Y., Nakamura, M., Umeda, M., Nishii, K., Mori, N., and Nishimoto, T. (2001) *Gene* (*Amst.*) **272,** 25–33
37. Kay, B. K., Williamson, M. P., and Sudol, M. (2000) *FASEB J.* **14,** 231–241
38. Kametaka, S., Shibata, M., Moroe, K., Kanamori, S., Ohsawa, Y., Waguri, S., Sims, P. J., Emoto, K., Umeda, M., and Uchiyama, Y. (2003) *J. Biol. Chem.* **278,** 15239–15245
39. Hu, X., Hicks, C. W., He, W., Wong, P., Macklin, W. B., Trapp, B. D., and Yan, R. (2006) *Nat. Neurosci.* **9,** 1520–1525
40. Willem, M., Garratt, A. N., Novak, B., Citron, M., Kaufmann, S., Rittger, A., DeStrooper, B., Saftig, P., Birchmeier, C., and Haass, C. (2006) *Science* **314,** 664–666
41. Kramer, S., Ozaki, T., Miyazaki, K., Kato, C., Hanamoto, T., and Nakagawara, A. (2005) *Oncogene* **24,** 938–944